Marine and Petroleum Geology 91 (2018) 519–531

Contents lists available at ScienceDirect

Marine and Petroleum Geology

journal homepage: www.elsevier.com/locate/marpetgeo

Research paper

Thermal impact of igneous sill-complexes on organic-rich formations and implications for petroleum systems: A case study in the northern Neuquén Basin, Argentina

J.B. Spacapan[a,*], J.O. Palma[b], O. Galland[c], R. Manceda[d], E. Rocha[e], A. D'Odorico[e], H.A. Leanza[f]

[a] YPF – CONICET, Argentina
[b] Y-TEC – CONICET, Argentina
[c] PGP, Department of Geosciences, University of Oslo, Norway
[d] Y-TEC, Argentina
[e] YPF, Argentina
[f] MACN-CONICET, Argentina

ARTICLE INFO

Keywords:
Sill-complex
Maturity
Source rock
Neuquén basin
Argentina

ABSTRACT

Numerous sedimentary basins in the world host voluminous igneous sill-complexes, i.e. stacking of sills that are emplaced in different levels of the sedimentary sequence. When sills are emplaced in organic-rich sedimentary formations, they can considerably affect the thermal and maturation history of the hydrocarbon source rock and can be highly relevant elements of the petroleum system. Most models of the thermal impacts of igneous sills on source rock consider one or few intrusions. However, the parameters that govern host rock maturation related to full sill-complexes remain unclear. In this contribution, we integrate borehole data and thermal 2D-modelling to quantify the temperature and maturation effects of a sill-complex in a 2D section on the sedimentary formations of the Neuquén basin, Argentina. In this basin, extensive magmatic activity took place during Oligocene-Miocene and upper Miocene age. There are numerous magmatic intrusions, dominantly sills, emplaced in organic-rich shale formations in the study area. Our modelling results show that (1) the source rock maturation in the study area was dominantly triggered by the sills, so that the area would be immature without the sills, (2) multiple sills have more pronounced thermal impact than a single, thick sill, (3) volumes of host rock between intrusions can have different degree of maturation depending on intrusion spacing, and (4) the temperature of the host rock at the time of sill emplacement controls to a great extent the thermal and maturation impact of the sills. Our work provides valuable insights into how the sills affected hydrocarbon generation during Oligocene-Miocene and Upper Miocene magmatic activity in the Neuquén basin. In addition, our study suggests that most of the kerogen has been transformed to hydrocarbon in areas where the sills are located.

1. Introduction

Numerous sedimentary basins worldwide host voluminous igneous intrusive complexes made of dikes, sills and laccoliths (e.g., Magee et al., 2016), which can affect the thermal state of sedimentary host rocks (Aarnes et al., 2010, and references therein). Local intrusion-induced maturation of sedimentary formations has been documented in, e.g. the Neuquén Basin in Argentina (Orchuela et al., 2003; Monreal et al., 2009), and in the Paraná Basin in Brazil (Thomaz Filho et al., 2008; Santos et al., 2009). When intrusive complexes are voluminous, basin-scale effects can be observed, i.e., in the Vøring Basin in the Norwegian margin (Fjeldskaar et al., 2008; Aarnes et al., 2015), the Karoo Basin in South Africa (Aarnes et al., 2011b) and the Tunguska Basin in Siberia (Svensen et al., 2009).

In many basins, numerous intrusions were preferentially emplaced in organic-rich formations (Monreal et al., 2009; Jackson et al., 2013). The interactions between igneous intrusions and their organic-rich host rocks can have major implications for the petroleum system: (1) the heating of organic-rich rocks can lead to the maturation, and even over-maturation, of organic matter and generation of hydrocarbons (Othman et al., 2001; Jones et al., 2007; Fjeldskaar et al., 2008; Delpino and Bermúdez, 2009; Monreal et al., 2009; Aarnes et al., 2015; Karvelas et al., 2015); (2) large volumes of hydrocarbons can be catastrophically released to the atmosphere and impact global climate (Svensen et al.,

* Corresponding author.
E-mail addresses: juan.b.spacapan@set.ypf.com (J.B. Spacapan), octavio.palma@ypftecnologia.com (J.O. Palma), olivier.galland@geo.uio.no (O. Galland), rene.e.manceda@set.ypf.com (R. Manceda), emilio.rocha@ypf.com (E. Rocha), alejandro.dodorico@ypf.com (A. D'Odorico), hleanza@macn.gov.ar (H.A. Leanza).

https://doi.org/10.1016/j.marpetgeo.2018.01.018
Received 8 August 2017; Received in revised form 4 January 2018; Accepted 14 January 2018
Available online 31 January 2018

2004; Aarnes et al., 2015); (3) structures induced by sill emplacement can generate fluid flow pathways or fluid traps (Cartwright et al., 2007; Rateau et al., 2013; Haug et al., 2017; Schmiedel et al., 2017) and (4) intrusions can be fractured hydrocarbon reservoirs (Bermúdez and Delpino, 2008; Monreal et al., 2009; Witte et al., 2012; Gudmundsson and Løtveit, 2014). This study will focus on how intrusions locally heat source rocks.

There is an extensive literature dealing with the thermal impact of igneous intrusions on their organic-rich host rocks, with particular focus on the extent of the thermal aureole, ranging mainly from 30% to 200% intrusion thickness (Simonet et al., 1981; Gilbert et al., 1985; Galushkin, 1997; Othman et al., 2001; Cooper et al., 2007; Thomaz Filho et al., 2008; Santos et al., 2009; Annen, 2011; Agirrezabala et al., 2014). However, they showed that sill intrusions can cause larger aureoles due to elevated background host rock temperatures, and a non-linear response 1:1 of aureole thickness to sill thickness can be expected. Most studies only take into account the thermal effect of one intrusion (see Aarnes et al., 2011a). Aarnes et al. (2011b) quantified how the thermal interactions between two sills can enhance maturation between the sills, depending on the vertical distance between them, affecting the thermal aureole extension. In addition, Fjeldskaar et al. (2008) considered the effects of more than 20 intrusions in the Vøring Basin, offshore Norway, and their implications in terms of host rock maturation. They modelled the thermal impact of multiple intrusions, and suggest that the sill-complex can trigger significant increase of kerogen cracking to hydrocarbon. All of these studies show that the thermal and maturation impacts of sill-complexes on petroleum systems are not trivial and depend on the sill-complex architecture and geological setting.

In this study, we aim to quantify the thermal and maturation impacts of a sill-complex on organic-rich host rocks, located in the Río Grande Valley, northern Neuquén Basin, Argentina (Fig. 1 A). Here, the host rocks of the sills are the main source rocks of the basin, i.e. the Vaca Muerta and Agrio Fms. Host rock maturation and hydrocarbon generation triggered by intrusions in the Neuquén Basin has been demonstrated by several authors (Uliana and Legarreta, 1993; Schiuma, 1994; Rossello et al., 2002; Orchuela et al., 2003; Delpino and Bermúdez, 2009; Monreal et al., 2009; Alberdi-Genolet et al., 2013). Also some authors documented sills as fractured reservoirs (Uliana and Legarreta, 1993; Schiuma, 1994; Rossello et al., 2002; Orchuela et al., 2003). However, a quantification of the thermal and maturation impacts of a whole sill-complex is currently lacking. Thus, the aims of our study are to (1) quantify the thermal impact of a sill-complex on the organic-rich formations, and (2) identify which parameters of the sill-complex influence the degree and distribution of host rock maturation and hydrocarbon generation.

2. Geological setting

The study area is located in the southern Mendoza province, west central Argentina, and belongs to the northern part of the Neuquén Basin (Fig. 1 A). This is a retroarc basin (Ramos, 1978), which extends between 32° and 40° S latitude, from the south of Mendoza province to the extra-andean region of Neuquén (Herrero Ducloux, 1946) covering an area of over 120.000 km^2 (Uliana and Biddle, 1988; Legarreta et al., 1993). The basin comprises a record of up to 7000 m of Late Triassic – Early Cenozoic deposits, the deposition of which was controlled by sea level changes and local tectonics of western Gondwana (Legarreta and Gulisano, 1989). The result was a discontinuous succession of continental and marine deposits that were accumulated in different cycles (Groeber, 1937), separated by several key unconformities (Leanza, 2009) (Fig. 1 B).

The Neuquén Basin was originated during Late Triassic-Early Jurassic as isolated rift depocenters, half-graben types, which were delimited by basement normal faults (Gulisano, 1981; Vergani et al., 1995; Franzese and Spalletti, 2001). They formed as a result of extensional tectonics associated with the break up of Pangea and of the negative subduction velocities in the western margin of Gondwana (Franzese and Spalletti, 2001).

During Middle Jurassic to Early Cretaceous, the isolated depocenters started to coalesce, forming a broad basin, due to a change to neutral subduction regime and the evolution of a volcanic arc. The basin sedimentation was dominated by thermal subsidence (sag stage) and eustatic sea-level changes, forming what is considered the classical filling of Mesozoic marine, evaporitic and continental rocks in northern Neuquén Basin (Gulisano and Pleimling, 1995). In southern Mendoza province, the sag stage resulted in the deposition of the Mendoza Group, which consists of: (1) the Tithonian - Early Valanginian Vaca Muerta Fm. (*ca.* 125–140 m thick), composed of bituminous shales, deposited under anoxic conditions of shelf and slope marine settings, characterized by a high organic matter content (TOC) from 3 to 8%, with peak values of 12% and dominant Type II kerogen (Sylwan, 2014); (2) the Middle Valanginian Chachao Fm. (ca 35–50 m thick), deposited above the Vaca Muerta Fm., consisting of a carbonate ramp full of biogenic material (Kozlowski et al., 1993; Brissón and Veiga, 1998); (3) the Late Valanginian - Early Barremian Agrio Fm. (*ca* 250–300 m thick)

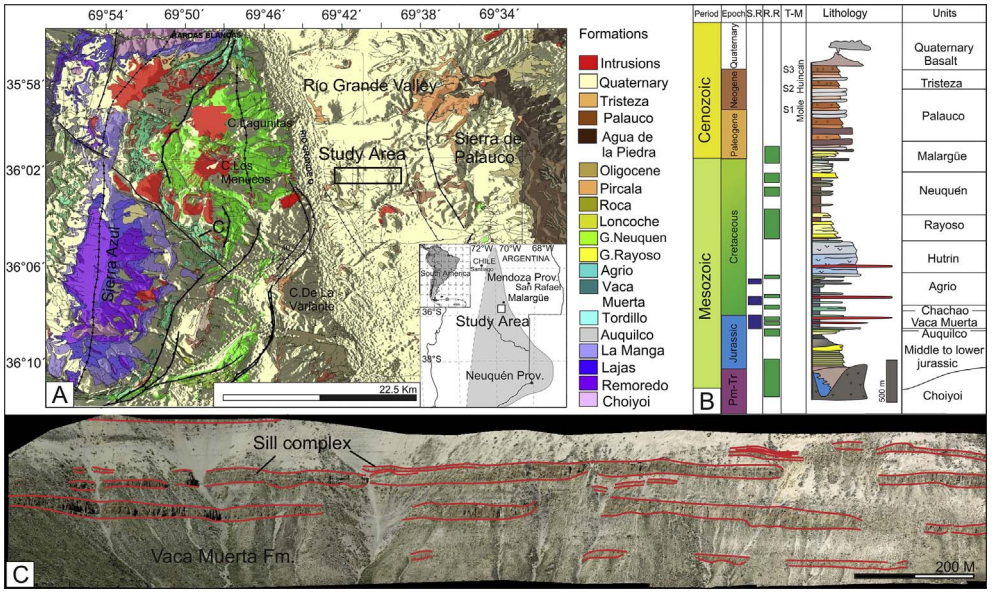

Fig. 1. A. Geological map of the Río Grande Valley area. Letter C accounts for outcrop picture from the next image. **B.** Sedimentary column for the Río Grande Valley. The main sills are hosted in the Agrio and Vaca Muerta organic-rich formations. S.R: source rock. R.R: reservoir rock. T–M: Tectono-magmatic events for southern Mendoza. S1, S2, and S3 are deformation events from Silvestro and Atencio (2009). Molle and Huincán are the eruptive cycles described by Combina and Nullo (2011). **C.** Ortho-rectified photograph of sill intrusions (outlined red) emplaced in the Vaca Muerta Fm., west of the study area. (For interpretation of the references to colour in this figure legend, the reader is referred to the Web version of this article.)

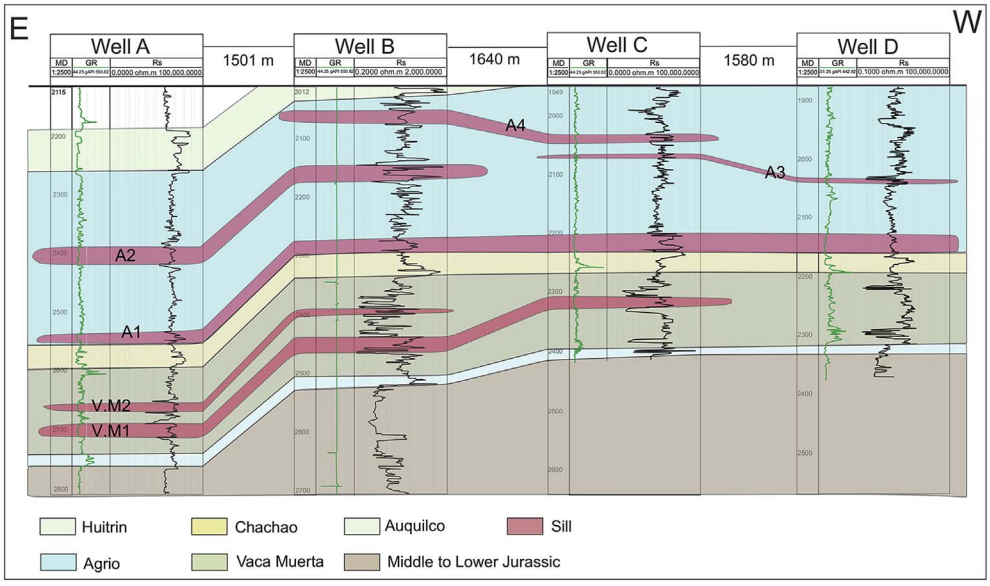

Fig. 2. Gamma ray (GR) and Resistivity (Rs) logs of Wells A-D used in this study. The logs display formation tops and lateral sill correlations (red) interpreted from cutting analyses. The sills are emplaced within the Agrio and Vaca Muerta source rocks. (For interpretation of the references to colour in this figure legend, the reader is referred to the Web version of this article.)

deposited as a transgressive organic-rich marly shale, with a TOC content from 2 to 3% and peak values up to 5% (Fig. 1 B). This Middle Jurassic-Early Cretaceous period was defined as post rift stage by Howell et al. (2005).

In the Early Cretaceous, the retroarc-sag phase ends and the tectonic regime transitionally changed to compressive, due to a decrease in the subduction angle and the beginning of the Andean orogeny (Cobbold and Rossello, 2003; Ramos et al., 2010) This produced the inversion of the normal faults of the Triassic rifts, developing fold and thrust belts in the retroarc (Manceda and Figueroa, 1995; Giambiagi et al., 2005; Folguera et al., 2006; Fennell et al., 2015). The associated depositional environments became restricted hypersaline marine with deposition of dolomite, gypsum, halite and silvinite and of continental fluvial and lacustrine sediments (Huitrín Fm.) (Vergani et al., 1995).

In the Late Cretaceous, the Neuquén Basin became a foreland basin and eastward migrations of the orogenic front produced the first syn-orogenic deposits (Cobbold and Rossello, 2003; Tunik et al., 2010). This occurs at approximately 100 Ma, with the deposition of several formations characterized by the continental red beds of the Neuquén Group. Subsequently, the Malargüe Group, including the Loncoche and Pircala Fms. separated from the Neuquén Group by an erosional unconformity, indicating an Atlantic marine ingression in the basin during Maastrichtian–Danian times.

Along with the development of the orogenic front, in the Late Cretaceous to Neogene, the basin experienced massive episodes of volcanism, both in the Neuquén Andes and the Neuquén Embayment (Kay et al., 2006). This volcanic activity resulted in the formation of the large back-arc volcanoes of Payún Matrú (Llambías et al., 2010), Tromen (Galland et al., 2007), Chachahuén (Kay et al., 2006), and Auca Mahuida (Rossello et al., 2002), as well as the vast volcanic plateau of the Payenia and the Huantraico syncline (Ramos and Folguera, 2005; Llambías et al., 2010).

Overall, this igneous activity lead to the formation of voluminous sill-complexes emplaced in the Mesozoic formations of the Neuquén Basin, in particular in the organic-rich shale of the Vaca Muerta and Agrio Fms. (Fig. 1 B and C). Numerous hydrocarbon fields in the basin are associated with these igneous sills (Schiuma, 1994; Rossello et al., 2002; Orchuela et al., 2003; Delpino and Bermúdez, 2009; Monreal et al., 2009; Alberdi-Genolet et al., 2013).

The study area is located in the Río Grande Valley, southern Mendoza Province, south of the Bardas Blancas village (Fig. 1 A). The valley is a morphologic depression with N-S orientation, bounded to the West by the basement-cored anticline of the Sierra Azul – Puntilla del Huincán and to the East by the Palauco, Cara Cura and Reyes ranges (Kozlowski et al., 1993). It belongs to the Malargüe Fold-and-Thrust Belt (Kozlowski et al., 1993; Manceda and Figueroa, 1995; Horton et al., 2016). Near the eastern side of the valley, the Los Cavaos anticline constitutes the most conspicuous feature (see Legarreta et al., 1985; Manceda and Figueroa, 1995; Giambiagi et al., 2009). The volcanic activity in the study area mainly occurred during the Late Oligocene-Middle Miocene Molle Eruptive Cycle (MEC) and the Late Miocene-Pliocene Huincán Eruptive Cycle (HEC), defined by Bettini (1982) and Combina and Nullo (2011) (Fig. 1 B). These eruptive cycles resulted in thick lava flow sequences, as well as numerous andesitic to basaltic sills dominantly emplaced in the source rock formations of the Mendoza Group (Fig. 1 B and C). Escribano et al. (1984, YPF internal report) dated an andesitic sill in the Vaca Muerta Fm., yielding a radiometric age of 22 Ma. Another sample from one sill located in Agrio Fm yielded an Ar-Ar cooling age of 10.5 Ma (Unpublished Repsol internal report, 2006). These radiometric ages suggest that the sills in the Río Grande Valley result from both the Oligocene to Early Miocene Molle Eruptive Cycle (MEC) and the Middle to Late Miocene Huincán Eruptive Cycle (HEC) (Nullo et al., 2002; Combina and Nullo, 2011) (Fig. 1 B). The sills emplaced in these organic-rich formations are the main fractured reservoirs of the hydrocarbon fields along the Río Grande Valley (Schiuma, 1994; Witte et al., 2012).

3. Methods

This study aims to quantify the thermal impact of sill-complexes on organic-rich shale formations through thermal modelling in the Río Grande Valley, northern Neuquén Basin (Fig. 1 A). This requires constraining the spatial distribution of the sills in the subsurface and the thermal properties of the rocks. To achieve this, our analysis integrates (1) borehole data from four wells owned by YPF (including cutting descriptions, rock cores, and well logs) and (2) Vitrinite, TOC and rock-eval pyrolysis data from another well in the near vicinity of the four wells. With this data, we constructed a detailed cross section of the studied sill-complex through well correlations. The four wells used in the analysis are named, from east to west, as A, B, C, and D (Fig. 2), and the well used for rock-eval pyrolysis is named E and is located 1 km to the north of well D. The wells are separated from each other by about 1500 m approximately.

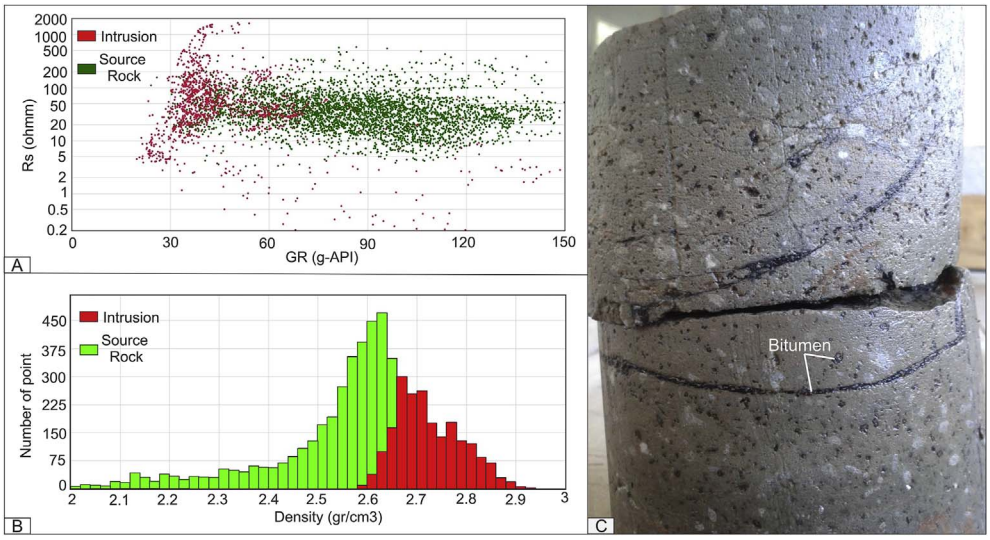

Fig. 3. A. Plot Rs vs GR logs displaying the typical behaviour of sills emplaced in the Vaca Muerta Fm. Sills exhibit high Rs and very low GR. **B**. Density plot for intrusions and source rock. Sills exhibit density values from 2.65 to 2.95. **C.** Photograph of core sample from andesitic sill, showing voids and fractures filled with bitumen.

3.1. Borehole data

The available open-hole log data from the four wells of the Río Grande Valley (A-D) includes resistivity (Rs) and gamma ray (GR) logs. The Rs and GR properties of magmatic sills are easily recognized in logs (Figs. 2 and 3A). They are characterized by rather high Rs and very low GR values, evidencing a tight igneous rock with little or no clay or potassium feldspar content. Average Rs is approximately 60 Ω m, but it can also reach values up to 100 Ω m in thicker intrusions (Fig. 3 A). The average values of GR are 37 GAPI for all the intrusions identified in the four wells, with maximum values of 60 GAPI.

These systematic Rs and GR characteristics of sills make their mapping in the logs straightforward and robust. In addition, the proposed interpretation of the sills is supported by cuttings analysis (YPF Internal Reports). This allows confident correlation and mapping of the lateral extent of theses igneous bodies throughout the Río Grande Valley (Fig. 2). The interpreted intrusions of the four wells were crosschecked against geological reports, drill cuttings and full diameter cores. Finally we perform a W-E geological cross section generated with the Move 2D software. We identified 6 main sheet-like intrusions, of different thickness, compositions, lengths and depths, emplaced in the Vaca Muerta and Agrio Fms. Note that high Rs and low GR values are present in the Huitrín Fm. and the Chachao Fm. (Fig. 2). These horizons are not interpreted as sills, as they correspond to well known and described carbonate formations, as supported by cuttings analyses (YPF internal reports).

Rs values for the host rock can greatly vary depending on the lithology, porosity and water salinity. The Neuquén Group has Rs values of 40 Ω m on average, whereas the Agrio and Vaca Muerta Fms. (Mendoza Group) have an average of 57.5 Ω m. GR values for the host rocks are strictly tied to lithology, mainly due to clay content.

3.2. Thermal modelling

The thermal effects of sills on the host rock maturation were modelled by the Easy %Ro equation from Sweeney and Burnham (1990), using the Petromode 2D software. Petromode 2D calculates the evolution of the temperature distribution resulting from heat diffusion associated with cooling intrusions. The resulting temperature fields allow to calculate theoretical values for temperature evolution around the sills, Vitrinite Reflectance (%Ro), Total Organic Carbon content (TOC), and the Transformation Ratio (TR), which is a measurement of the amount of cracked kerogen. Note that our thermal models do not account for heat advection by fluid flow (Iyer et al., 2017).

The original TOC contents of the host rock formations were measured from geochemical analyses of immature samples, with values of 6%–3% for the Vaca Muerta Fm. and 2.4% for the lowermost part of the Agrio Fm. Initial Hydrogen Indexes (HI) values are of 600 mgHC/gTOC for the Agrio Fm. and 675 mgHC/gTOC for Vaca Muerta Fm. In addition, the thermal model was calibrated using porosity, permeability, capillary pressures and bottom-hole temperatures from wells A-D. We used specific kerogen kinetics obtained by analysis of the Agrio and Vaca Muerta source rocks to model the transformation from organic matter to hydrocarbon. Some values of Vitrinite Reflectance (% Ro) from Well E were used to compare with theoretical Easy %Ro (Sweeney and Burnham, 1990) values generated from 2D model simulations.

Our thermal modelling accounts for the two magmatic emplacement events described by Combina and Nullo (2011). However, because we do not have the ages of all the sills identified from well data, we simplify the model by assigning the intrusions in the Vaca Muerta Fm. to the first magmatic event (MEC), while intrusions in Agrio Fm. were assigned to the second magmatic pulse (HEC). Two main sill compositions were determined based on petrographic descriptions of core and cutting samples (YPF internal report), being five sills of andesitic compositions, and one of basaltic composition (see section 4.1 and Fig. 3B). We assumed an initial temperature of 1200 °C for the basaltic sill, and 1100 °C for the andesitic ones. In addition, we used the following parameters for intrusions: thermal conductivity of 2.60 W/m/K, solidus temperature of 850 °C, magma density of 2.45 gr/cm^3, heat capacity of 10.88 MJ/kg/K and crystallization heat of 700 MJ/m^3. We used the same values of thermal properties for both compositions because of the lacking data for andesitic sills. The time steps for calculation were of 500 years, for a total geologic time of 199.5 Ma. Importantly, the thermal modelling also includes burial history in the study area, based on age, thickness, and lithology of each sedimentary formation constrained from cutting analysis.

3.3. Host rock geochemistry

In order to validate the modelling of the thermal impact of intrusions on source rocks, TOC contents and Rock-Eval analyses were performed from 32 samples from the Agrio Fm. and 26 samples from the Vaca Muerta Fm. The samples were collected from Well E (not included in cross section), located 1 km to the north of well D, where cutting sampling was possible. Rock-Eval pyrolysis evaluates petroleum potential, including generation, thermal maturity and type of organic matter of the source rocks. This analysis has been widely used to evaluate the thermal impact of intrusions on organic-rich host rocks (Simoneit et al., 1978; Clayton and Bostick, 1986; Bishop and Abbott,

1995; Othman et al., 2001; Aarnes et al., 2011b; Alalade and Tyson, 2013; Agirrezabala et al., 2014). Samples with TOC values greater than 0.5% for shales and 0.3% for carbonates were considered adequate for rock-eval pyrolysis. We use different pyrolysis parameters, such as Hydrogen Indexes (HI) and Maximum temperature (Tmax). The values of HI are proportional to the amount of hydrogen content within the kerogen and are expressed in mgHC/gTOC. Tmax (°C) is the temperature of the maximum hydrocarbon generation rate. Additionally we use few values of Vitrinite Reflectance from the Vaca Muerta Fm., and few from the Agrio Fm., to calibrate the model.

4. Results

4.1. Lateral sill correlation

Intrusions mapping and lateral correlation was conducted using Rs and GR values from borehole data. The intrusions mapped on the section exhibit typical dominantly concordant sheet-like shape, i.e. sills. We identified six sills with different thickness, compositions, lengths and depths, emplaced both in the Vaca Muerta and Agrio Fms. (Figs. 2 and 3 A).

In well A, we identified four intrusions, one in the upper part of the Agrio Fm. (A2 in Fig. 2 and Fig. 4), another one between Agrio and Chachao Fms. (A1 in Fig. 4), and the other two in the Vaca Muerta Fm. (VM1 and VM2 in Fig. 4). The upper and lower intrusions in the Agrio Fm. are 27 m thick and 13 m thick, respectively (A1 and A2 in Fig. 4). The two sills emplaced in the Vaca Muerta Fm. display a thickness of 22 m for the lower one (VM1) and 9 m for the upper one (VM2). The vertical distance between VM1 and VM2 is 36 m, between VM2 and A1 is 100 m, and between A1 and A2 is 140 m.

In Well B, the sedimentary sequence is 200 m shallower than in well A. Here, three intrusions are hosted in the Agrio Fm. and two in the Vaca Muerta Fm. (Figs. 2 and 4). In the Agrio Fm., the upper intrusion is 26 m thick, and was defined as a new sill named A4. The middle sill is 27 m thick and was correlated with sill A2, previously identified in well A. The lower intrusion on the Agrio Fm. is 13 m thick, and was emplaced along the contact with the Chachao Fm., so that it was correlated with sill A1. In the Vaca Muerta Fm., the upper sill has a thickness of 6 m and was correlated with sill VM2, and the lower one has a thickness of 22 m thick and was correlated with sill VM1. The vertical distance between VM1 and VM2 is 47 m, between VM2 and A1 is 96 m, between A1 and A2 is 94 m, and between A2 and A4 is 64 m.

Well C exhibits 3 intrusions located in the Agrio Fm. and one in the Vaca Muerta Fm. (Figs. 2 and 4). The upper intrusion in the Agrio Fm. is 17 m thick and was correlated with sill A4. The middle one is 4 m thick only, and was identified as a new sill named A3. The lower sill is 30 m thick and is emplaced along the Agrio-Chachao discontinuity, so that it was correlated with sill A1. The sill identified in the Vaca Muerta Fm. is correlated with the lower sill identified in Wells A and B, i.e. VM1. The vertical distance between VM1 and A1 is 87 m, between A1 and A3 is 130 m, and between A3 and A4 is 25 m.

Finally, in the well D there are two intrusions in the Agrio Fm. The upper intrusion is 3 m, and is correlated with the thin A3 intrusion identified in Well C (Figs. 2 and 4). The second intrusion, located at the Agrio-Chachao discontinuity, is 33 m thick and is correlated with sill A1. The vertical distance between A3 and A4 is 92 m.

4.2. Thermal modelling results

In order to quantify the thermal effects of the sill-complex, we compared results from 2D thermal modelling of the mapped regional section (1) without intrusion and (2) with the intrusions mapped in the Agrio and Vaca Muerta Fms.

4.2.1. Thermal modelling without intrusions

In this model we assume that from 199.5 Ma to present day, temperature and maturity increased only because of burial (Fig. 5 A). In the lower part of the Lower Jurassic units, theoretical %Ro values are 0.7–1%, indicating maturation in the main oil window. In the mid-Lower Jurassic formations (Vaca Muerta Fm.) to mid-Agrio Fm., maturity is of 0.55–0.7 %Ro, i.e. indicating maturation in the early oil window (Fig. 5 A). The formations shallower than the mid-Agrio Fm. are immature, with Ro values from 0 to 0.5%.

The reference model without intrusions (Fig. 5A) shows a relatively homogeneous lateral maturity distribution. To the west, the Agrio Fm. is early mature. To the east, the younger Huitrín Fm. is early mature because of deeper burial.

The calculated temperature field at present-day in the Lower Jurassic units would be 110 °C, while the temperatures in Vaca Muerta and Agrio Fms. would range between 100 and 80 °C (Fig. 5 B). Some parts of the Vaca Muerta Fm. would develop Transformation ratios (TR) between 20 and 40% during Miocene (Fig. 5 C).

4.2.2. Thermal modelling with intrusions

The first emplacement event occurs at 22 Ma, where two intrusions (VM1 and VM2) were emplaced in the mid- and lower parts of the Vaca Muerta Fm. (Fig. 6 A). 500 years after the emplacement of this first magmatic event, local thermal anomalies are observed in the vicinity of the intrusions (Fig. 6 A). The thermal aureole (112–480 °C) extends upward to the lower and mid parts of the Agrio Fm. However, in parts where the intrusions overlap, the thickness of the thermal anomaly extends more below the intrusions than above. The highest temperatures occurred in the 60 m thick host rock in between VM1 and VM2 intrusions, reaching values of 434–480 °C (Fig. 6 A).

A second magmatic event of the Upper Miocene was modelled using an age of 10.5 Ma for the multiple intrusions (A1, A2, A3 and A4)

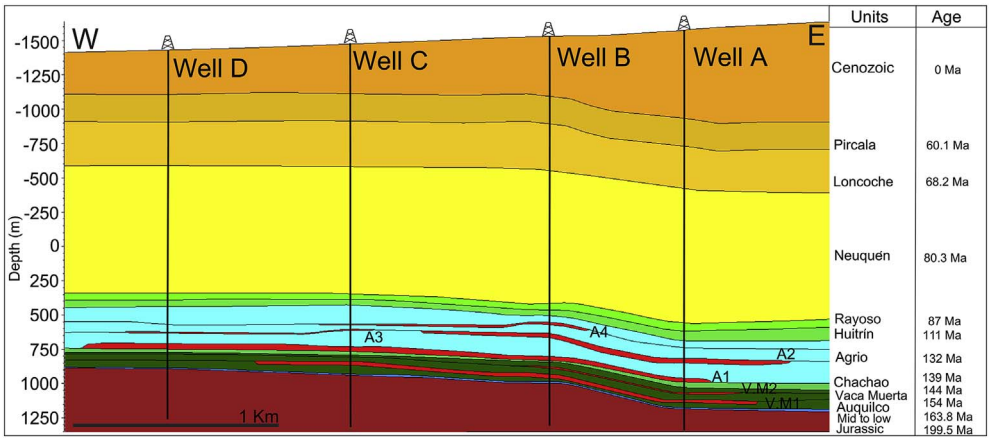

Fig. 4. Geological cross section of the study area. Mapping of sedimentary units and sills integrated borehole data and geological control reports. The thickness of sedimentary column tends to increase toward the eastern part of section.

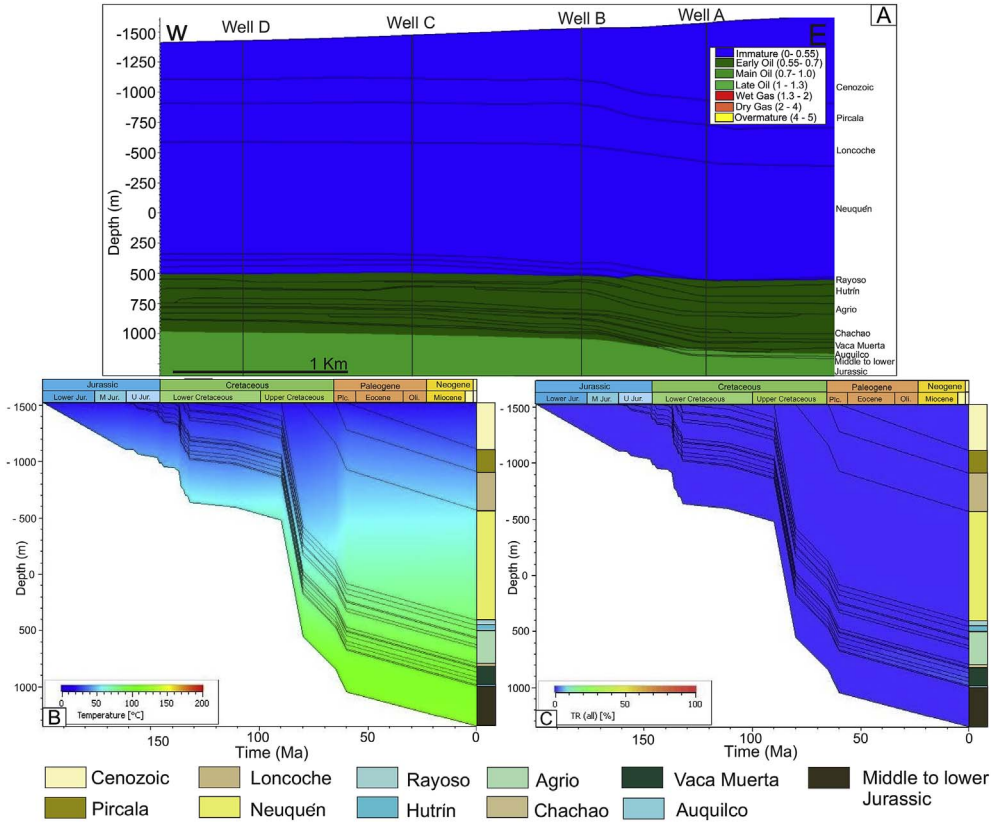

Fig. 5. A. Map of theoretical Vitrinite Reflectance (%Ro) distribution along the studied geological cross section at present day without intrusion. Lower Jurassic units would reach the Main Oil for, whereas the Agrio and Vaca Muerta Fms. would reach the early oil window (%Ro from 0.55 to 0.7). **B**. Plot of 1D temperature profile through time from 199.5 Ma to present day, without intrusions. Maximum temperatures of 100 °C are calculated in the Lower Jurassic to the Vaca Muerta Fm. from Miocene. **C**. Plot of 1D Transformation Ratio (TR) profile through time from 199.5 Ma to present day, without intrusion. Only a low percentage of organic matter is cracked to hydrocarbons in the Vaca Muerta Fm. since Miocene.

emplaced in the Agrio Fm. (Fig. 6 B). We assumed that at this time, the two sills emplaced in the Vaca Muerta Fm. were already cooled, and that no temperature anomaly is associated with them. 500 years after the emplacement of the second intrusive event, thermal anomalies also concentrate around the intrusions, similar to those resulting from the first magmatic event. The thermal anomaly associated with this second event exhibits a more irregular distribution than that associated with the first event. In the western and eastern parts, where two intrusions are present, the thermal anomaly extends upward to the top of the Agrio Fm. In addition, the distribution of the thermal anomaly between the intrusions is rather complex. In the west part of the section, between sills A3 and A1, the temperatures reach 342° to 388 °C (Fig. 6 B). The middle part of the section is more complex because of the local overlapping of three intrusions, the group A1, A3, A4 to the west, and the group A1, A2, A4 to the east. There, the maximum temperatures reach 434° to 480 °C. The overlapping of the three sills also widens the thermal anomaly to the middle part of the Neuquén Group, with temperature values of 158°–204 °C. In the middle part of the section, where only two sills overlap (A1 and A4), the thermal anomaly is reduced, with maximum temperature values of only 204 °C (Fig. 6 B).

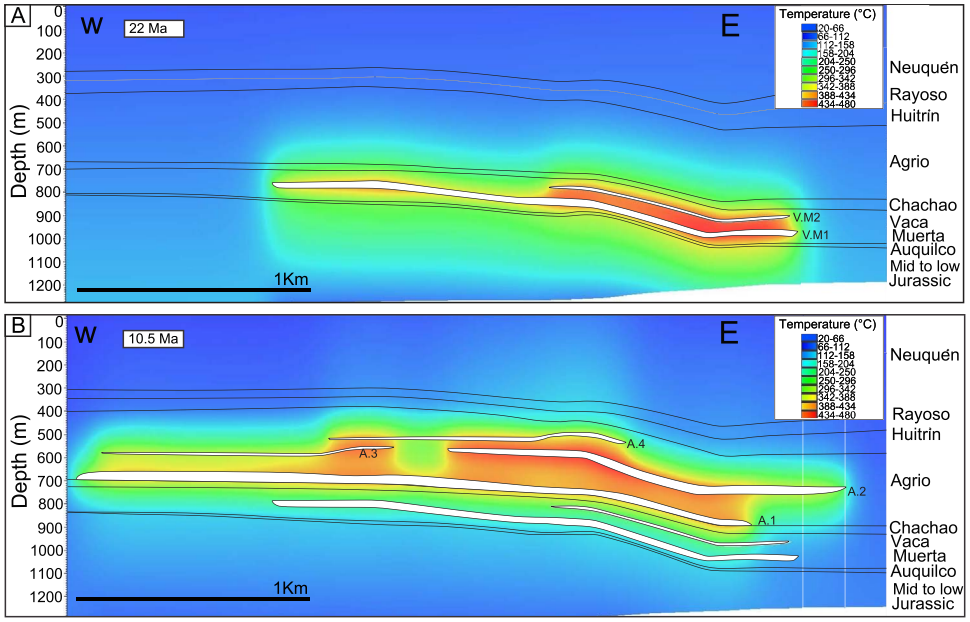

Fig. 6. A. Map of temperature distribution along the studied cross section 500 years after to the first magmatic event, i.e. sills emplaced in the Vaca Muerta Fm. at 22 Ma. **B.** Map of temperature distribution along the studied cross section 500 years after to the second magmatic event, i.e. sills emplaced in the Agrio Fm. at 10.5 Ma. Note that this profile does not include the thermal effect of the first magmatic event.

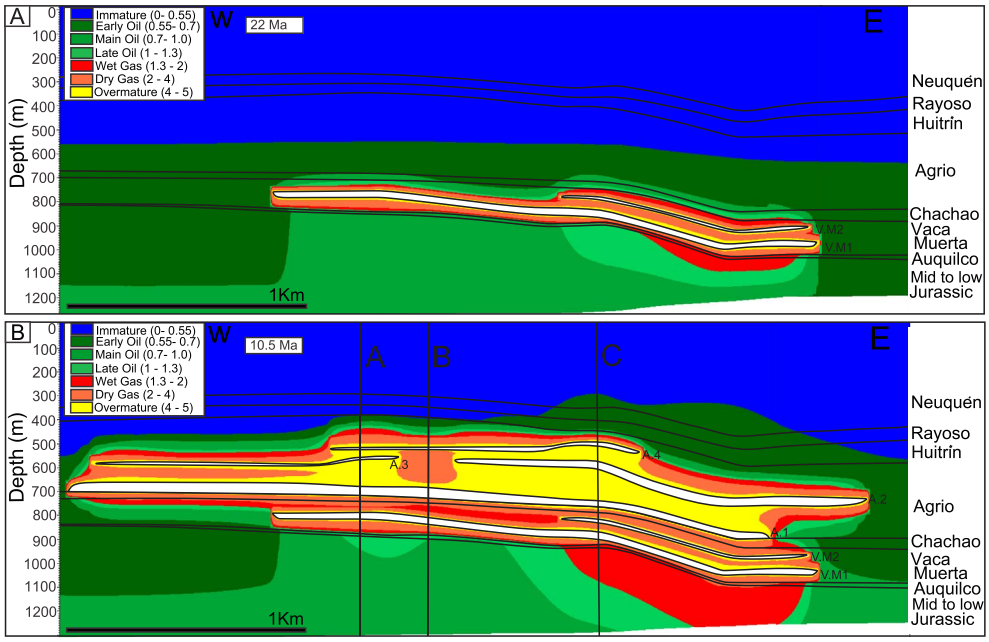

Fig. 7. A. Map of Vitrinite Reflectance distribution, and associated maturation, along the studied cross section 500 years after the first magmatic event, i.e. sills emplaced in the Vaca Muerta Fm. at 22 Ma. **B.** Map of Vitrinite Reflectance distribution, and associated maturation, along the studied cross section 500 years after the second magmatic event, i.e. sills emplaced in the Agrio Fm. at 10.5 Ma.

The thermal modelling also calculates vitrinite reflectance maps, which allow evaluating the maturity evolution associated with the sill-complex (Fig. 7A and B). The size and distribution of the thermal anomalies associated with the two magmatic events triggered various degrees of maturation on the intruded organic-rich host rock. 500 years after the first intrusion event, the %Ro degree shows a good correlation with the extent of the associated thermal anomaly, as it can be seen from Figs. 6 A and 7 A. In the mid–western parts, where only the lower thick intrusion (VM1) is present in the Vaca Muerta Fm., an extensive area below the sill reached the main oil window, with values of 0.7–1 % Ro, whereas the extent of the main oil window above the intrusion is only 30 m thick (Fig. 7 A). The domain of the late oil window (1–1.5 % Ro) exhibits similar thickness below and above the intrusion. The domains in the wet gas (1.3–2 %Ro) and dry gas (2–4 %Ro) windows are 40 m thick on average. In addition, an overmature aureole only extends 10 m around the intrusion. In the eastern part of the section, where two intrusions overlap (VM1 and VM2), the aureole of maturation is much thicker and exhibits a more complex distribution than in the west (Fig. 7 A). The late oil window aureole attains a maximum thickness of 180 m below the intrusions, while above them it is only 25 m thick (Fig. 7 A). Similarly, the wet gas window aureole is thicker below (95 m) than above (30 m) the intrusions. The dry gas window aureole is symmetrical above and below the intrusions, with an average thickness of 40 m, and includes the block of host rock sandwiched between the intrusions. An overmature aureole has a major extent between the intrusions, but is thinner below the lower intrusion (17 m) and above the upper intrusion (10 m) (Fig. 7 A).

Nearly 500 years after the second magmatic event, maturity distribution is very complex (Fig. 7 B). In the western part, where three intrusions (A1, A3, A4) are emplaced in the Agrio Fm. (Fig. 7 B, profile A), the whole host rock thickness in between the intrusions is overmature (Fig. 8 A). Locally, in the central part of the section (Fig. 7 B, profile B), where only two intrusions in the Agrio Fm. overlap (A1 and A4), most of the host rock is in the dry gas window (Fig. 8 B). The eastern part of the section contains the maximum number of intrusions (VM1, VM2, A1, A2, and A4) (Fig. 7 B, profile C). Here the maturity anomaly attains the maximum thickness (Fig. 8 C), with the wet gas and late oil window aureoles extending downward to great portions of the Jurassic units. Additionally, above the five sills, the early oil window aureole reaches its maximum vertical extent to the middle of the Neuquén Group (Fig. 7 B).

Fig. 9 A displays the calculated maturity distribution at present day. It exhibits an irregular shape, reaching its maximum vertical extent (uppers units of Neuquén Group) in the middle part of the section, and thinning towards the eastern and western parts (Fig. 9 A). The maximum vertical extent of the maturation field is consistent with areas where there are more overlapping intrusions (5 intrusions along profile B; Fig. 9 B). The Lower Jurassic units exhibit well-developed late oil and main oil windows aureoles, as well as a wet gas window aureole in the central and eastern parts of the section. Along the whole section, significant dry gas window aureoles have been developed between the intrusions located in the Vaca Muerta Fm. (Fig. 9 A and 11 A). Large overmature domains are confined between the intrusions hosted in some parts of the Agrio Fm. (Fig. 9 A). In contrast, in areas with no intrusions %Ro are lower, ranging 0.7–1 (Fig. 9 C).

At present-day, in the Vaca Muerta and the lower Agrio Fms., TR reaches values of 80–100% in areas intruded by sills (Figs. 10 A and 11 B). Furthermore, there is a gradual lateral decrease of TR values away from intrusions tips. In contrast, in the zones without intrusions, the TR values only attain 5% to 20% (Fig. 11 B).

TOC concentration map at present-day (Fig. 12) shows that high proportions of the original organic matter of the Agrio and Vaca Muerta Fms. were cracked in areas intruded by sills. In the lowermost Agrio Fm., TOC decreases from 3 to 0.7%, whereas in the upper Agrio Fm. it decreases down to 0.2%. Additionally, the Vaca Muerta Fm. exhibits a strong decrease of TOC % in areas close to the intrusions. The TOC % also decreases from 6.8 to 2.7% in the lowermost Vaca Muerta Fm. (Fig. 13 A). Similar behaviour is shown by the HI, decreasing in magnitude towards the intrusions.

4.3. Total organic carbon and rock-eval Hydrogen Index

In this study, we also quantify the thermal impact of the multiple sheet-like intrusions on the TOC, HI and Tmax values in the Vaca Muerta and Agrio Fms. based on cutting chemical analysis from well E (Fig. 14).

In the studied Well E, the Agrio Fm. hosts five intrusions, the thickness of which are, from top to bottom, 5 m, 18 m, 6 m, 3 m and 10 m (Fig. 14 A). The total organic carbon (TOC) concentration in cutting samples is variable. However, a general behaviour can be observed, suggesting a decrease of TOC content close to the intrusions (Fig. 14 A). In the upper part of the Agrio Fm., TOC values range from

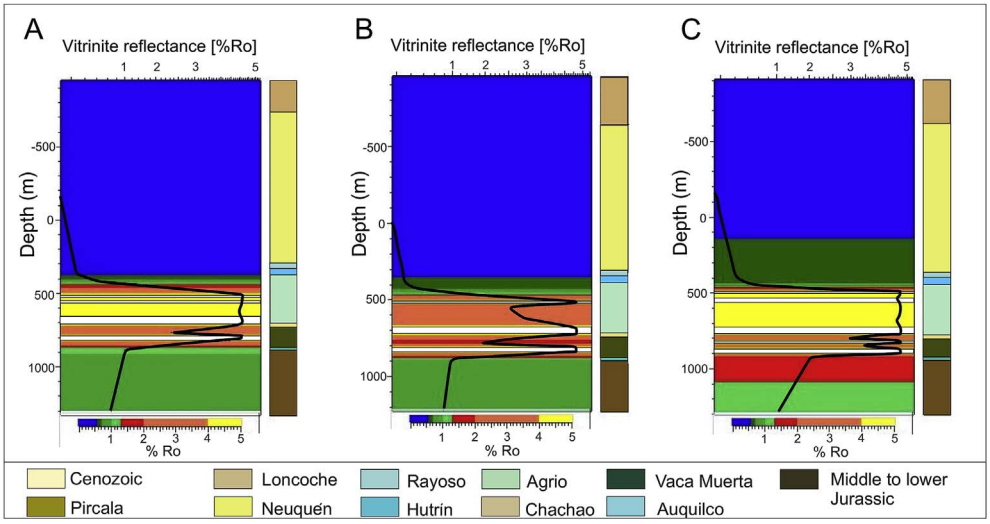

Fig. 8. Plots of vitrinite reflectance profiles 500 years after the second magmatic episode (see profile locations in Fig. 7). Maximum extent of maturity is in Profile C, i.e. where there are more intrusions.

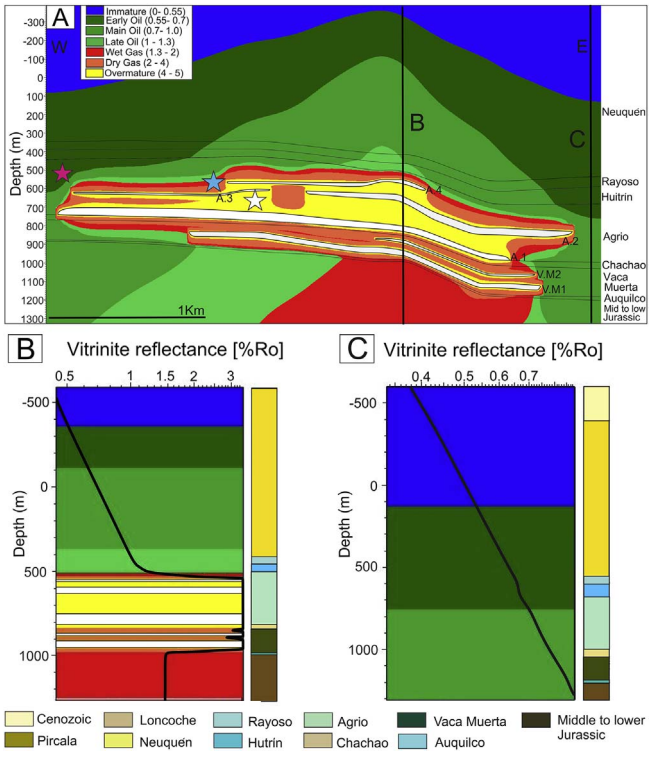

Fig. 9. A. Map of Vitrinite Reflectance distribution, and associated maturation, induced by intrusions along the studied cross section at present-day. Pink, light blue and white stars locate the data displayed in Fig. 12. **B**. Plot of vitrinite reflectance profile B in central part of map in A, where there is a higher superimposition of intrusives. **C**. Plot of vitrinite reflectance profile C in eastern part of map in A, where there is no intrusive. Note that there is more maturation compared with Fig. 5A (i.e., where maturation is only generated by burial) due to a lateral thermal effect of intrusives. (For interpretation of the references to colour in this figure legend, the reader is referred to the Web version of this article.)

1% to 2%, while those closer to the intrusions vary from 0.6% to 1.6%. The TOC percentage increases from the mid-to lower section of the sedimentary column, attaining maximum values of 3.8%. Closer to the intrusions TOC values tend to decrease again.

Hydrogen Index (HI) shows a consistent pattern in the plot of Fig. 14 A, with a pronounced decrease on HI values close to and between the sills. In the upper part of Agrio Fm., background values of HI range from 430 to 350 mgHC/gTOC, but towards the upper intrusion they decrease notably to values of 15 mgHC/gTOC. A similar behaviour occurs between the intrusions that are located in the middle part of the sedimentary column, where HI is of 19–78 mgHC/gTOC, with some exceptions. In the lower part of the column (2190 m), the HI increases from 250 to 320 mgHC/gTOC, and decreases again downward to values of 20 mgHC/gTOC in contact with the lower intrusion (2268 m).

Tmax has a constant behaviour for Agrio Fm., with average values from 422 to 433 °C. However, there are lower Tmax values (410 °C) between the intrusions in the mid-Agrio Fm. and lowest Tmax values in the lowermost Agrio Fm., above the lower intrusion (402 °C at 2245 m).

Some Vitrinite Reflectance values show a strong maturation between the intrusions in the mid-Agrio Fm. from 2 to 1.5 %Ro (wet gas window) (Fig. 14 A). However, in the uppermost part of the Agrio Fm., one value of 0.6 %Ro was obtained suggesting maturation in the early oil window.

The Vaca Muerta Fm. hosts three intrusions, the thickness of which are, from top to bottom, 5 m, 2 m and 30 m (Fig. 14 B). The pyrolysis parameters reveal a similar behaviour close to the intrusions than in the Agrio Fm. Close to the upper thin intrusions (2330 m and 2347 m), TOC values are somewhat constant, with average values of 2.8%. However, the TOC content strongly decreases at the upper (2370 m) and lower (2400 m) contacts of the thickest sill, with values down to 1%. In the upper part of the Vaca Muerta Fm., above and between the thin sills, HI is 22 mgHC/gTOC on average. In addition, in the upper and lower contacts of the thickest intrusion, HI slightly decreases. Tmax is variable in the upper part of the Vaca Muerta Fm., whereas on the upper and lower contacts of the thick intrusions, Tmax displays a significant increase from 416 to 420 °C.

Vitrinite Reflectance values (green circles) show a high maturation between the intrusions in the mid-Vaca Muerta Fm. from 3.5 %Ro (Dry gas field) (Fig. 14 B). Additionally, ~38 m below the thick intrusion (2438 m), one value reaches 1.8 %Ro (Wet gas window), while at 2477 m one vitrinite sample show a 1.1 %Ro (Late oil window).

5. Interpretation

Our models allow us to quantitatively assess the thermal impact and associated maturity produced by andesitic sills intruded in the sedimentary sequences of the northern Neuquén Basin, especially on the Vaca Muerta and Agrio Fms.

The models with and without intrusions show drastic differences in temperature and maturation patterns. Without intrusion, the shallowest maturation depth at present day is the base of the Huitrín Fm., with values of 0.55–0.7 %Ro, indicating early oil generation in Vaca Muerta and Agrio Fms. (Fig. 5). In addition, only a very limited percentage of organic matter is cracked to hydrocarbons (TR 30% on average) in the Vaca Muerta Fm. (Fig. 5 C). With intrusions, however, the Vaca Muerta

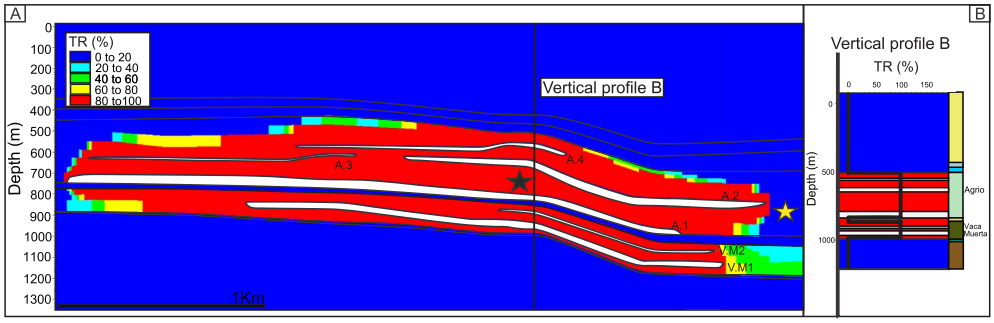

Fig. 10. A. Map of Transformation Ratio (TR) induced by intrusions along the studied cross section at present day. Black and yellow stars make reference to Fig. 11 B. **B**. Vertical profile of Transformation Ratio (TR) in the central part of section in A. Transformation Ratio for the Vaca Muerta and Agrio Fms. range from 80 to 100% where the intrusions are superimposed, and decreases moving away from the intrusions. (For interpretation of the references to colour in this figure legend, the reader is referred to the Web version of this article.)

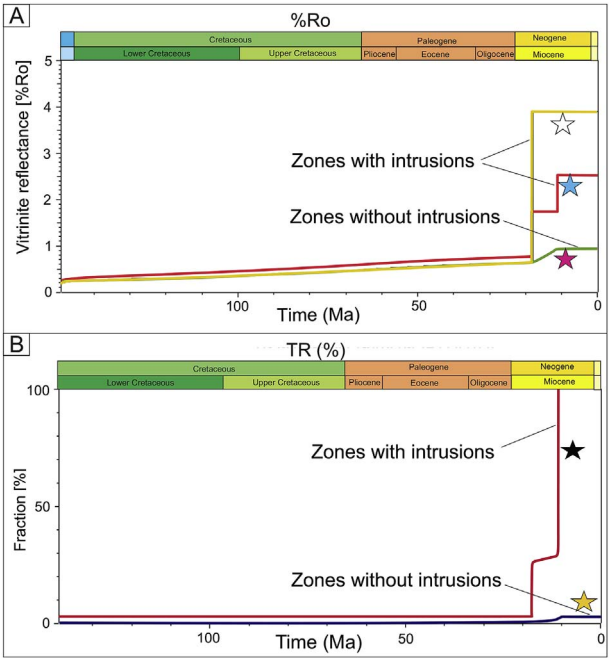

Fig. 11. A. Plot of Vitrinite Reflectance through time in a zone without intrusion (pink star), and in two zones affected by the sills (light blue and white stars). See Fig. 9 A for star's location. **B**. Transformation Ratio through time plot in a zone without intrusion (light brown star) and in a zone between intrusions (black star). See Fig. 10 A for star's location. (For interpretation of the references to colour in this figure legend, the reader is referred to the Web version of this article.)

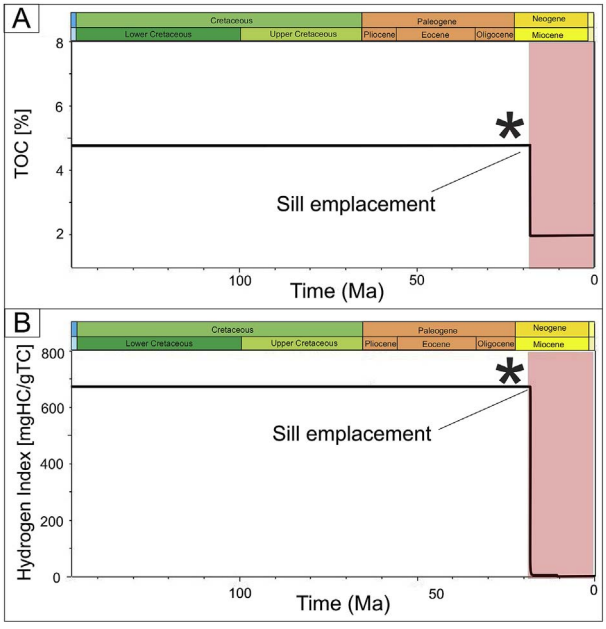

Fig. 13. A. Plot of TOC through time in the Vaca Muerta Fm. It shows an abrupt TOC decrease from 4.8% to 2.1% at the Lower Miocene, i.e. at emplacement of the first magmatic event. Black asterisk make reference to Fig. 12. **B**. Hydrogen Index (HI) plot through time in the Vaca Muerta Fm. It also shows an abrupt HI decrease at the Lower Miocene. Black asterisk make reference to Fig. 12.

and Agrio Fms. reach the main oil to dry gas maturation windows (Figs. 7–9 and 11 A). The highest degrees of maturity and the highest transformation ratios (80%–100%) are concentrated in the surroundings of the sills. Further from the intrusions, the Vaca Muerta and Agrio Fms. exhibit lower degrees of maturation and lower Transformation Ratios, ranging 2–25% (Figs. 10 and 11 B). These results show that the source-rock maturation in the studied area was dominated by the igneous intrusions, and that the maturation of the source rock formations was constrained in the intruded domains.

Fig. 6 displays a complex temperature distribution associated with the studied sill-complex, both at small and large scale. At small scale, i.e. at the sill scale, the higher temperatures and higher degrees of maturation are restricted to the source rock domains in between sills of significant thickness (Figs. 6 and 7). This is visible in the eastern part of the sill-complex emplaced in the Vaca Muerta Fm. (Fig. 6 A) and in the central part of the sill-complex emplaced in the Agrio Fm. (Fig. 6 B). At large scale, i.e. at the scale of the whole sill-complex, the thickest maturation aureole in the central part of the section occurs where the highest number of intrusions is emplaced (Fig. 11). We conclude that the vertical superposition of sills significantly enhances source-rock

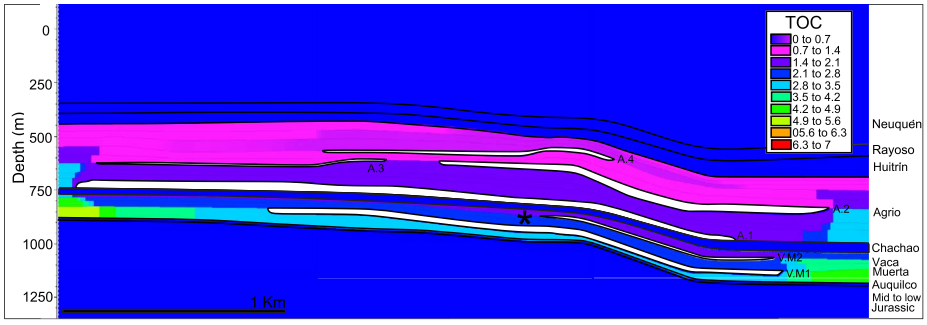

Fig. 12. Map of TOC content along studied cross section at present day, after maturation induced by intrusions. TOC% values tend to decrease in areas where the intrusions are located. Black asterisk makes reference to Fig. 13.

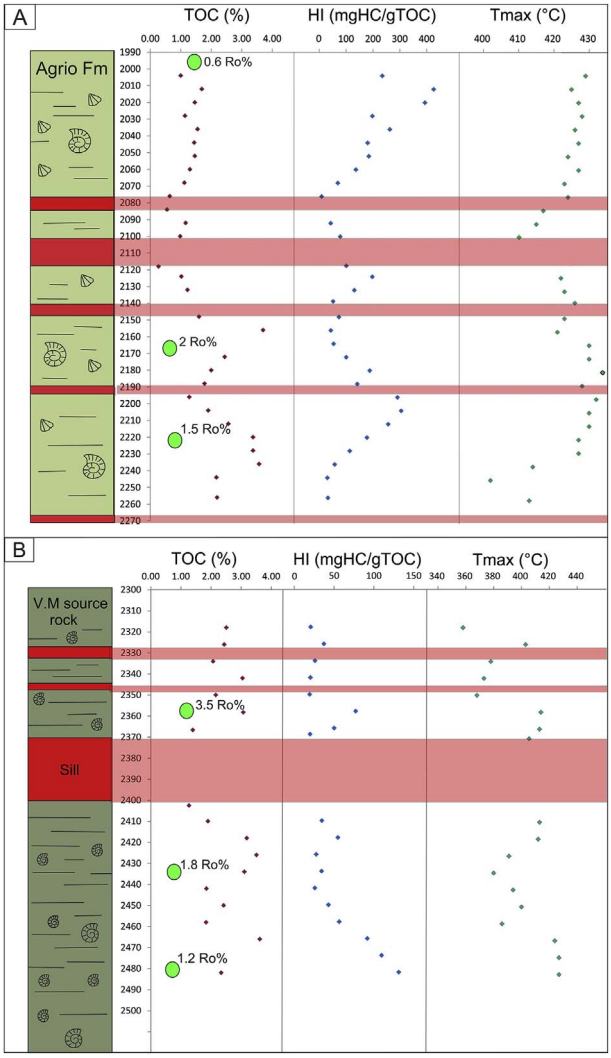

Fig. 14. Profiles of TOC, HI and Tmax measured across the Agrio Fm. (A) and Vaca Muerta Fm. (B) intruded by sills (red) in well E, located 1 km to the north of Well D. Green circles are real %Ro values measured in core samples. **A.** TOC content tends to decrease toward the sills contacts. However, some high levels of TOC concentration can be found between intrusions, likely a very rich organic matter facies. HI displays a general decrease toward the sills. Tmax shows an increase close to the intrusions; however, some values (2100 m) tend to decrease toward the intrusions. **B**. For the upper thin sills, the TOC contents show no trend toward the sills contacts. Conversely, toward the thick sill (2370 m), the upper and lower contacts show a significant decrease of TOC content. HI displays strong decrease toward the thick sill. Tmax reach the maximum temperatures of 418 °C on the upper and lower contacts of the thick sill. (For interpretation of the references to colour in this figure legend, the reader is referred to the Web version of this article.)

maturation between the sills, and that the extent of the maturation aureole is enhanced by the local number of intrusions.

Figs. 7 and 9 exhibit complex maturation distributions associated with the studied sill-complex. Domains hosting several thin (< 7 m) and closely spaced intrusions tend to develop great overmatured areas, while domains with fewer amounts of intrusions tend to generate maturation in the dry gas window. Furthermore, if the sill-complex is dominated by thick (17 m), closely spaced intrusions, larger zones of overmaturation (100–150 m) can be generated in the host rock. Conversely, wet and dry gas can be developed if the sill-complex consists of intrusions of different thickness (3–40 m), since the thermal effect decreases and host rock is not completely burnt.

Our results show some variability of the thermal impact of the intrusions with respect to depth. Fig. 6 A shows that the overall thermal anomaly is thicker (150 m) below the sills emplaced in the Vaca Muerta Fm. than above. In addition, in the domain intruded by the two sills in the Vaca Muerta Fm. (VM1 and VM2), the thermal anomaly is thicker (100–160 m) in the eastern part than in the western part (50–70 m), i.e. where the sills are deeper (Fig. 6 A). Similar observation is highlighted in the maturity map of Figs. 7 and 9, where the wet gas and dry gas fields are thicker (215–300 m) where the superposed sills emplaced in the Vaca Muerta Fm. are deeper. This suggests that the extent of the maturation triggered by the sills is strongly influenced by the temperature of the host rock due to sedimentary burial at the time of emplacement. The modelled maturation is extensive because the host rock temperature was high enough, i.e. the host rock was already in the early oil maturation window. Consequently, it is likely that the temperature anomaly induced by the first intrusive event strongly influenced the thermal and maturation impact of the second intrusive event. This likely explains the shallow extent of the maturation area (700 m) above the sill complex up to mid-Neuquén Fm. (Fig. 9 A), whereas without sills the upper Agrio Fm. should be immature (Fig. 5 A). All these results show that the thermal impact of intrusions depends to a great extent on the previous background temperature of the host rock, whether the temperature results from sedimentary burial or from earlier intrusions. Quantifying the thermal and maturation impacts of sill-complexes on sedimentary sequences therefore requires a good understanding of their burial evolution.

The thermal modelling results can be interpreted in terms of maturation of the Vaca Muerta and Agrio source rocks. The modelled TOC and HI (Fig. 13) behaviour is similar to that obtained by TOC and Rock-Eval pyrolysis measurements from cutting samples of well E (Figs. 14 and 15). The strong decrease of TOC and IH values (Figs. 14 and 15) close to the thick sills emplaced in the Vaca Muerta and Agrio Fms. shows that the heat diffused from the sills considerably enhanced the cracking of the organic matter, subsequently released as volatile compounds, in the vicinity of the sills. In addition to these local effects, the current average of the TOC (2.5%) and HI (< 50 mgHC/gTC) in the Vaca Muerta Fm. are substantially lower than their initial values of ~5% and ~700 mgHC/gTC, respectively. This shows that the sills triggered substantial maturation of the organic matter in the whole thickness of the Vaca Muerta Fm. Vitrinite reflectance data shows values corresponding to wet to dry gas maturation in areas between the intrusions in the Vaca Muerta and Agrio source rocks. However, some differences can be found between theoretical vitrinite and real vitrinite data, since the number, size and distribution of sills in well E are different than those in the studied cross section. These differences between real and theoretical maturation can be related to sill thickness distribution. The average sill thickness in the studied cross section is 29.5 m, while the average sill thickness in well E is 10.14 m only. Therefore, some differences can be found on the degree of organic matter maturation between well E and the modelled cross section.

To summarize, the complexity and variation of the parameters, such as sill thickness distribution, sill spacing, intrusion timing, number of intrusions, background temperature, and host rock thermal properties, can have a strong impact on the extent and degree of host rock maturation.

6. Controls on aureole thickness and study limitations

The 2D modelling results and cutting sample analyses show that temperature distribution and host rock maturation are strongly influenced by the sill-complex. Our models, based on the Easy %Ro equation (Sweeney and Burnham, 1990), cannot calculate %Ro values higher than ≃4.66 (Hantschel and Kauerauf, 2009). This limitation of the model has already been discussed by Fjeldskaar et al. (2008), who argue that ≃4,5%Ro limit is not a natural limit, and that it is beyond the upper limit of thermogenic gas generation, so it is beyond the realm of interest for many basin researchers.

Our simulations only account for heat conduction, not advection by fluid flow, similarly to the models of Fjeldskaar et al. (2008) and Aarnes

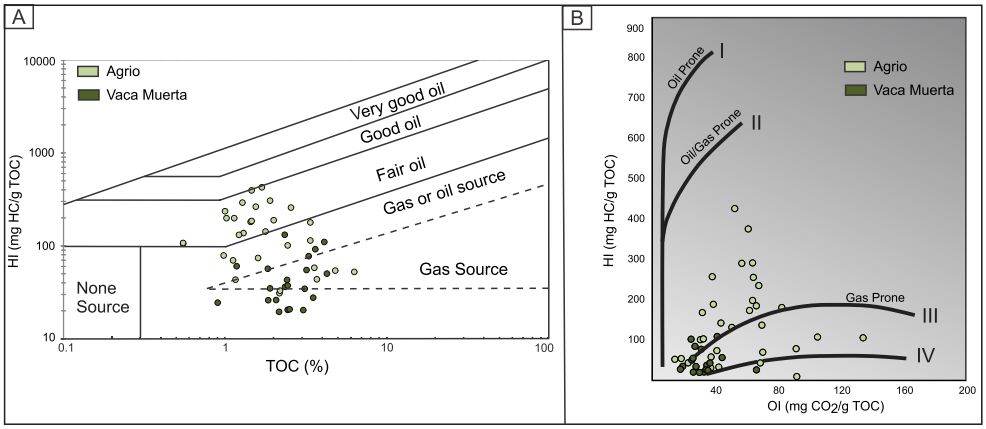

Fig. 15. A. Source Rock Richness plot for Agrio and Vaca Muerta samples (well E) as a function of Hydrogen Index (HI) and wt % TOC. Poorly metamorphosed samples in Agrio Fm. top show a fairly good oil potential. Contrary, in samples between sills and those close to them HI and TOC values decrease, suggesting that great portion of organic matter was cracked during metamorphism. Additionally, most Vaca Muerta Fm. samples correspond to gas source type, while the rest are to a large degree barren. **B**. Modified van Krevelen diagram indicating dominantly Type II kerogen for samples. Most samples of Vaca Muerta and Agrio Fms. are affected by thermal maturation and have low HI and OI values. In particular, Vaca Muerta Fm. samples show a HI decrease from 657 mgHC/gTOC (Vaca Muerta initial HI content) to 33.68 mgHC/gTOC on average.

et al. (2010). In low permeability rocks (1 mD), such as in the Vaca Muerta and Agrio Fms. (1–1.5 mD; YPF internal reports), it is a fair assumption, as discussed by Wang and Manga (2015), who modelled aureole geometries in host rocks of different permeabilities. Their result showed that symmetrical aureoles are developed in low permeability rocks, where convection is depreciable. We cannot rule out, however, the occurrence of fracturing induced by pore pressure induced by organic matter maturation (Kobchenko et al., 2011; 2013). This process can locally significantly increase rock permeability, and so fluid flow and associated heat advection (Iyer et al., 2017) However, systematic measurements of symmetrical aureoles around the studied intrusions (unpublished data) strongly suggest that upward heat advection is very limited.

In our model, we consider concordant sheet intrusions (sills), which are the most common intrusion types in the study area (Schiuma, 1994). In this geometry, the heat diffusion is dominantly normal to the sills and the resulting thermal and maturation patterns are sub-parallel to the sills (Fig. 7). There could be also sills which are not intersected by the boreholes used in this study, and therefore not incorporated into the models. Our results are different than those of Monreal et al. (2009), who modelled the host rock maturation and hydrocarbon generation induced by the cooling of laccolithic intrusions (concordant dome-shaped intrusions which produce bending and/or failure of the overlaying strata) in the south of the Río Grande Valley. Because of the drastic difference in intrusion shapes, the resulting maturation distributions substantially differ.

In our models, we consider two intrusive events in Lower Miocene and Upper Miocene, constrained by Ar-Ar datings (Escribano et al., 1984, YPF internal report; Nullo et al., 2002; Repsol internal report, 2006). The models highlight how these two intrusive episodes triggered complex, two-stage evolution of the maturation in the studied area (Fig. 9). This is compatible with the organic geochemistry and fluid inclusion data of Alberdi-Genolet et al. (2013), which show that two pulses of hydrocarbon generation occurred in the Río Grande Valley area. These authors argue that the first and second pulses of hydrocarbon generation resulted from burial and the subsequent Oligocene-Miocene magmatic event, respectively. Our results suggest instead, that the pulses of hydrocarbon generation can result from the Lower Miocene and Upper Miocene intrusive episodes, respectively. Even if the thermal models without intrusion show some maturation because of burial, it is of much lower magnitude with respect to maturation induced by the intrusions. Note, additionally, that Eocene intrusions of 35.5 Ma (Escribano et al., 1984, YPF internal report) were also emplaced in the Agrio Fm., in the southern part of the Río Grande Valley. This suggests that some earlier pulses of local host rock maturation could have occurred during this Eocene magmatic event. The variability of the intrusive's age could have major implications on the maturity degree of the host rocks. This is consistent with the results of Sydnes et al. (2018), who demonstrated that timing of sills emplacement have a major implication on host rock maturation. However, the timing of the considered intrusions in our model cannot be better constrained due to the lack of datable core samples of intrusives.

Aarnes et al. (2010) show that the thickness of the aureole induced by a single sill in a normal geothermal gradient is 1–1.5 times the thickness of the sill. Our models, however, calculate aureoles that are much thicker. Several reasons can explain this difference. First, we show that when successive events of magma emplacement happened, the first event increases the background temperature of the host rock. When the following magmatic events occur, the background temperature is higher, corresponding to a local abnormally elevated geothermal gradient, and the resulting thickness of the maturation aureoles are higher, as also observed by Aarnes et al. (2010) and Annen (2011, 2017). Similarly, the background temperature also varies with the burial depth at the time of emplacement: our models show that deeper sills develop thicker aureoles. Second, our results show that multiple sills trigger much more thermal impact than a single sill. Indeed, the interaction between the thermal aureoles of the sills is not linear, leading to a maturation aureole between the sills that is much larger than the summed thickness of the aureoles of each individual sill (Figs. 6 and 7). This is in good agreement with the results of Aarnes et al. (2011b), who demonstrate that the interactions between thermal aureoles of two sills become stronger when the vertical distance between the sills decreases.

Raymond and Murchison (1991) also discuss the effect of sill composition on their thermal impact. The variability in the thermal properties of the intrusion's composition, especially the thermal diffusivity, can influence the aureole size, as demonstrated by Annen (2017). The Petromode software accounts for the following thermal properties of the intrusions: temperature of emplacement, solidus temperature, thermal conductivity (which depends on thermal diffusivity), magma heat capacity and crystallization heat. We ran different simulations changing these parameters and the results were very similar. The parameter that most affected the models was the temperature of emplacement, while the others had minor effects. We used the thermal properties of basalts because those of andesites are poorly constrained. This assumption has minor influence on the modelling results, and we foresee that our main conclusions remain valid. However, the constrain of the thermal properties of andesites and other compositions will be important for a better calibration of the models.

In this work, as in previous ones from other authors (Jones et al., 2007; Fjeldskaar et al., 2008; Monreal et al., 2009; Aarnes et al., 2010, 2015; Iyer et al., 2013; Wang et al., 2013; Wang and Manga, 2015; Iyer et al., 2017; Svensen et al., 2017; Sydnes et al., 2018), we implemented only 1D and 2D models of the thermal impact caused by igneous intrusions. The main reason is that the 3D architecture of the studied sill-complex is not well constrained. However, the 3D architecture of sill-

complexes can have some implications on the extension and degree of maturation especially in the presence of associated fluid flow (Aarnes et al., 2011a; Iyer et al., 2017; Kjoberg et al., 2017). Nevertheless, given that igneous sills are concordant intrusions that extend over large distances, the heat diffusion is dominantly normal to the sills, thus we consider that 2D, even 1D, models, are good approximations of the first-order thermal effects of the sills; the third dimension would provide only more detailed, second-order results.

Our models and cutting samples analyses show that the thermal impact of the studied sill-complex enhances the Transformation Ratio of the kerogen to hydrocarbons (locally up 80%–100%). Our results show, therefore, that the sills dominantly triggered the generation of the hydrocarbons produced in the oil field. This is consistent with the results of Fjeldskaar et al. (2008) and Sydnes et al. (2018), who demonstrate that sill swarms could more than double the kerogen fraction transformed to hydrocarbon. We prove that the emplacement of a sill-complex in organic-rich shale can be the main triggering for hydrocarbon generation (see also Galushkin, 1997).

In the study area, the hydrocarbon generation resulting from the emplacement of igneous sills has lead to a profitable oil field, the reservoirs of which are the sills themselves (Schiuma, 1994; Monreal et al., 2009; Witte et al., 2012). Our study could therefore have significant implications for hydrocarbon exploration in the numerous volcanic basins worldwide, in which intrusive complexes are emplaced in organic-rich formations.

7. Conclusions

We address the thermal and maturation impacts of igneous sills on source rock formations in the northern Neuquén Basin, Mendoza Province, Argentina. The study integrates borehole data, well logging and geochemical data, which are used as inputs for 2D thermal modelling. The following points summarize the main conclusions of our study.

- The 2D model simulations show that the thermal architecture and source rock maturation in the Río Grande Valley are dominantly triggered by the sill-complex. Without sills, the source rock formations would be immature to marginally mature.
- We showed that the thermal impact depends on the sill-complex architecture. Parameters such as number of sills, sill spacing, sill thickness, sill composition and length, greatly affect the temperature distribution in the basin. Also, the host rock background temperature, prior to the sill emplacement, has a significant impact on the extent and degree of host rock maturation. Therefore, the knowledge of the burial history of the organic-rich formations is essential for quantifying the thermal and maturation impacts of the sill-complex.
- Another relevant factor that affects the degree of host rock maturation is the intrusions timing. An early intrusion episode increases the background temperature of the host rock, which can significantly enhance the thermal maturation impact of subsequent intrusion episodes.
- Our models suggest that two local pulses of hydrocarbon generation in the Río Grande Valley could have occurred during the Oligocene-Miocene and Middle-upper Miocene magmatic events. However, some Eocene ages for intrusions recorded to the southern of the study area could suggest a pulse of local hydrocarbons generation older than in our model.

To conclude, our study suggests that the thermal impact of sill-complexes can have great positive implications on petroleum systems in numerous worldwide basins. Our conclusions can thus have major implications for hydrocarbon exploration in volcanic basins.

Acknowledgements

Spacapan's salary is covered by a CONICET-YPF Foundation grant (Grant 2282014000359600). The authors are grateful to YPF (Grant 30-54668997-9) for funding the fieldwork, providing subsurface data and the advanced training for Spacapan. We thank to I. Brissón (YPF), M. Fasola (YPF) and R. Manoni (YPF-IAPG) for the important ideas and discussion that contributed to this manuscript. We acknowledge the very constructive reviews by Craig Magee and anonymous reviewer.

References

Aarnes, I., Svensen, H., Connolly, J.A., Podladchikov, Y.Y., 2010. How contact metamorphism can trigger global climate changes: modeling gas generation around igneous sills in sedimentary basins. Geochem. Cosmochim. Acta 74, 7179–7195.
Aarnes, I., Fristad, K., Planke, S., Svensen, H., 2011a. The impact of host-rock composition on devolatilization of sedimentary rocks during contact metamorphism around mafic sheet intrusions. Geochem. Geophys. Geosyst. 12.
Aarnes, I., Svensen, H., Polteau, S., Planke, S., 2011b. Contact metamorphic devolatilization of shales in the Karoo Basin, South Africa, and the effects of multiple sill intrusions. Chem. Geol. 281, 181–194.
Aarnes, I., Planke, S., Trulsvik, M., Svensen, H., 2015. Contact metamorphism and thermogenic gas generation in the Vøring and Møre basins, offshore Norway, during the Paleocene–Eocene thermal maximum. J. Geol. Soc. 172, 588–598.
Agirrezabala, L.M., Permanyer, A., Suárez-Ruiz, I., Dorronsoro, C., 2014. Contact metamorphism of organic-rich mudstones and carbon release around a magmatic sill in the Basque-Cantabrian Basin, western Pyrenees. Org. Geochem. 69, 26–35.
Alalade, B., Tyson, R.V., 2013. Influence of igneous intrusions on thermal maturity of Late Cretaceous shales in the Tuma well, Chad Basin, NE Nigeria. J. Afr. Earth Sci. 77, 59–66.
Alberdi-Genolet, M., Cavallaro, A., Hernandez, N., Crosta, D., Martinez, L., 2013. Magmatic events and sour crude oils in the Malargüe area of the Neuquén Basin, Argentina. Mar. Petrol. Geol. 43, 48–62.
Annen, C., 2011. Implications of incremental emplacement of magma bodies for magma differentiation, thermal aureole dimensions and plutonism–volcanism relationships. Tectonophysics 500, 3–10.
Annen, C., 2017. Factors affecting the thickness of thermal aureoles. Front. Earth Sci. 5.
Bermúdez, A., Delpino, D.H., 2008. Concentric and radial joint systems within basic sills and their associated porosity enhancement, Neuquén Basin, Argentina. Geol. Soc. Lond. Spec. Publ. 302, 185–198.
Bettini, F., 1982. Complejos efusivos terciarios presentes en las Hojas 30c y 32b (Puntilla del Huincán y Chos Malal), del sur de Mendoza y Norte del Neuquén, Argentina. In: Actas V Congreso Latinoamericano de Geología, pp. 79–114.
Bishop, A., Abbott, G., 1995. Vitrinite reflectance and molecular geochemistry of Jurassic sediments: the influence of heating by Tertiary dykes (northwest Scotland). Org. Geochem. 22, 165–177.
Brissón, I., Veiga, R., 1998. La estratigrafía y estructura de la Cuenca Neuquina. Gira de campo, Buenos Aires, Repsol YPF (unpublished report).
Cartwright, J., Huuse, M., Aplin, A., 2007. Seal bypass systems. AAPG Bull. 91, 1141–1166.
Clayton, J., Bostick, N., 1986. Temperature effects on kerogen and on molecular and isotopic composition of organic matter in Pierre Shale near an igneous dike. Org. Geochem. 10, 135–143.
Cobbold, P., Rossello, E., 2003. Aptian to recent compressional deformation, foothills of the Neuquén Basin, Argentina. Mar. Petrol. Geol. 20, 429–443.
Combina, A.M., Nullo, F., 2011. Ciclos tectónicos, volcánicos y sedimentarios del Cenozoico del sur de Mendoza-Argentina (35°-37° S y 69° 30'W). Andean Geol. 38, 198–218.
Cooper, J.R., Crelling, J.C., Rimmer, S.M., Whittington, A.G., 2007. Coal metamorphism by igneous intrusion in the Raton Basin, CO and NM: implications for generation of volatiles. Int. J. Coal Geol. 71, 15–27.
Delpino, D.H., Bermúdez, A.M., 2009. Petroleum systems including unconventional reservoirs in intrusive igneous rocks (sills and laccoliths). Lead. Edge 28, 804–811.
Escribano, D., Labayén, I., Rosso, M., Tozzi, A., Sanchez, M.C., Angelozzi, G. y, Spalletti, A., 1984. Estudio petrográfico, radimétrico, geoquímico y micropaleontológico de la secuencia sedimentaria infrayacente a la F. Huitrín e intrusivos asociados presentes en la Cuenca Neuquina surmendocina. Informe Inédito YPF.
Fennell, L.M., Folguera, A., Naipauer, M., Gianni, G., Vera, E.A.R., Bottesi, G., Ramos, V.A., 2015. Cretaceous deformation of the southern Central Andes: synorogenic growth strata in the Neuquén Group (35 30 0–37 S). Basin Res. 1, 22.
Fjeldskaar, W., Helset, H., Johansen, H., Grunnaleite, I., Horstad, I., 2008. Thermal modelling of magmatic intrusions in the Gjallar Ridge, Norwegian Sea: implications for vitrinite reflectance and hydrocarbon maturation. Basin Res. 20, 143–159.
Folguera, A., Ramos, V.A., Díaz, E.F.G., Hermanns, R., 2006. Miocene to quaternary deformation of the Guañacos Fold-and-thrust belt in the Neuquén Andes between 37 S and 37 30′ S. Geol. Soc. Am. Spec. Pap. 407, 247–266.
Franzese, J.R., Spalletti, L.A., 2001. Late Triassic–early Jurassic continental extension in southwestern Gondwana: tectonic segmentation and pre-break-up rifting. J. S. Am. Earth Sci. 14, 257–270.
Galland, O., Hallot, E., Cobbold, P.R., Ruffet, G., de Bremond D'Ars, J., 2007. Volcanism in a compressional Andean setting: a structural and geochronological study of Tromen volcano (Neuquén province, Argentina). Tectonics 26.

Galushkin, Y.I., 1997. Thermal effects of igneous intrusions on maturity of organic matter: a possible mechanism of intrusion. Org. Geochem. 26, 645–658.
Giambiagi, L., Alvarez, P.P., Bechis, F., Tunik, M., 2005. Influencia de las estructuras de rift triásico-jurásicas sobre el estilo de deformación en las fajas plegadas y corridas de Aconcagua y Malargüe, Mendoza. Rev. Asoc. Geol. Argent. 60, 662–671.
Giambiagi, L., Ghiglione, M., Cristallini, E., Bottesi, G., 2009. Características estructurales del sector sur de la faja plegada y corrida de Malargüe (35-36 S): distribución del acortamiento e influencia de estructuras previas. Rev. Asoc. Geol. Argent. 65, 140–153.
Gilbert, T.D., Stephenson, L.C., Philp, R.P., 1985. Effect of a dolerite intrusion on triterpane stereochemistry and kerogen in Rundle oil shale, Australia. Org. Geochem. 8, 163–169.
Groeber, P., 1937. Mapa Geológico de la Hoja 30c (Puntilla de Huincán) del mapa Geológico General de la República Argentina. Dirección Nacional de Mineria y Geologia.
Gudmundsson, A., Løtveit, I.F., 2014. Sills as fractured hydrocarbon reservoirs: examples and models. Geol. Soc. Lond. Spec. Publ. 374, 251–271.
Gulisano, C., 1981. El Ciclo Cuyano en el norte de Neuquén y sur de Mendoza. In: Congreso Geológico Argentino, pp. 579–592.
Gulisano, C., Pleimling, A.G., 1995. Field Guide the Jurassic of the Neuquén Basin: B. Secretaría de Minería de la Nación, Mendoza Province.
Hantschel, T., Kauerauf, A.I., 2009. Fundamentals of Basin and Petroleum Systems Modeling. Springer Science & Business Media.
Haug, Ø.T., Galland, O., Souloumiac, P., Souche, A., Guldstrand, F., Schmiedel, T., 2017. Inelastic Damage as a Mechanical Precursor for the Emplacement of Saucer-shaped Intrusions.
Herrero Ducloux, A., 1946. Contribución al conocimiento geológico del Neuquén extraandino. Bol. Inf. Pet. 23, 245–281.
Horton, B.K., Fuentes, F., Boll, A., Starck, D., Ramirez, S.G., Stockli, D.F., 2016. Andean stratigraphic record of the transition from backarc extension to orogenic shortening: a case study from the northern Neuquén Basin, Argentina. J. S. Am. Earth Sci. 71, 17–40.
Howell, J.A., Schwarz, E., Spalletti, L.A., Veiga, G.D., 2005. The Neuquén basin: an overview. Geol. Soc. Lond. Spec. Publ. 252, 1–14.
Iyer, K., Rüpke, L., Galerne, C.Y., 2013. Modeling fluid flow in sedimentary basins with sill intrusions: implications for hydrothermal venting and climate change. Geochem. Geophys. Geosyst. 14, 5244–5262.
Iyer, K., Schmid, D.W., Planke, S., Millett, J., 2017. Modelling hydrothermal venting in volcanic sedimentary basins: impact on hydrocarbon maturation and paleoclimate. Earth Planet Sci. Lett. 467, 30–42.
Jackson, C.A., Schofield, N., Golenkov, B., 2013. Geometry and controls on the development of igneous sill–related forced folds: a 2-D seismic reflection case study from offshore southern Australia. Geol. Soc. Am. Bull. 125, 1874–1890.
Jones, S., Wielens, H., Williamson, M.C., Zentilli, M., 2007. Impact of magmatism on petroleum systems in the Sverdrup Basin, Canadian Arctic Islands, Nunavut: a numerical modelling study. J. Petrol. Geol. 30, 237–256.
Karvelas, A., Magee, C., Shtukert, O., Schenk, O., Devine, T., 2015. Understanding magmatic history and its implications upon petroleum systems of the NE Rockall Basin. In: 77th EAGE Conference and Exhibition 2015.
Kay, S.M., Burns, W.M., Copeland, P., Mancilla, O., 2006. Upper Cretaceous to Holocene magmatism and evidence for transient Miocene shallowing of the Andean subduction zone under the northern Neuquén Basin. Geol. Soc. Am. Spec. Pap. 407, 19–60.
Kjoberg, S., Schmiedel, T., Planke, S., Svensen, H.H., Millett, J.M., Jerram, D.A., Galland, O., Lecomte, I., Schofield, N., Haug, Ø.T., 2017. 3D structure and formation of hydrothermal vent complexes at the Paleocene-Eocene transition, the Møre Basin, mid-Norwegian margin. Interpretation 5, SK65–SK81.
Kobchenko, M., Hafver, A., Jettestuen, E., Galland, O., Renard, F., Meakin, P., Jamtveit, B., Dysthe, D.K., 2013. Drainage fracture networks in elastic solids with internal fluid generation. Europhys. Lett. 102. http://dx.doi.org/10.1209/0295-5075/102/66002.
Kobchenko, M., Panahi, H., Renard, F., Dysthe, D.K., Malthe-Sorenssen, A., Mazzini, A., Scheibert, J., Jamtveit, B., Meakin, P., 2011. Fracturing controlled primary migration of hydrocarbon fluids during heating of organic-rich shales. J. Geophys. Res. – Solid Earth 116. http://dx.doi.org/10.1029/2011JB008565.
Kozlowski, E., Manceda, R., Ramos, V., Ramos, V., 1993. Estructura, Geología y Recursos Naturales de Mendoza. In: Relatorio del 12 Congreso Geológico Argentino y 2 Congreso de Exploración de Hidrocarburos, vol. I. pp. 235–256 (18).
Leanza, H.A., 2009. Las principales discordancias del Mesozoico de la Cuenca Neuquina según observaciones de superficie. Rev. Mus. Argent. Ciencias Nat. 11, 145–184.
Legarreta, L., Gulisano, C., 1989. An álisis estratigráfico secuencial de la Cuenca Neuquina (Triá sico SuperioreTerciario Inferior, Argentina), Simposio de Cuencas Sedimentarias Argentinas. Cuencas Sedimentarias Argentinas. In: 10 Congreso Geoló gico Argentino (Tucumá), Actas, pp. 22.
Legarreta, L., Kokogián, D., Boggetti, D., Kozlowski, E., Cruz, C., Rebay, G., 1985. Sierra de Palauco: Estratigrafía y estructura. YPF, Provincia de Mendoza unpublished report.
Legarreta, L., Gulisano, C., Uliana, M., Ramos, V., 1993. Las secuencias sedimentarias jurásico-cretácicas. In: Congreso Geológico Argentino.
Llambías, E.J., Bertotto, G.W., Risso, C., Hernando, I., 2010. El volcanismo cuaternario en el retroarco de Payenia: una revisión. Rev. Asoc. Geol. Argent. 67, 278–300.
Magee, C., Muirhead, J.D., Karvelas, A., Holford, S.P., Jackson, C.A., Bastow, I.D., Schofield, N., Stevenson, C.T., McLean, C., McCarthy, W., 2016. Lateral magma flow in mafic sill complexes. Geosphere 12, 809–841.
Manceda, R., Figueroa, D., 1995. Inversion of the Mesozoic Neuquén Rift in the Malargüe Fold and Thrust Belt, Mendoza, Argentina.
Monreal, F.R., Villar, H., Baudino, R., Delpino, D., Zencich, S., 2009. Modeling an atypical petroleum system: a case study of hydrocarbon generation, migration and accumulation related to igneous intrusions in the Neuquen Basin, Argentina. Mar. Petrol. Geol. 26, 590–605.
Nullo, F.E., Stephens, G.C., Otamendi, J., Baldauf, P.E., 2002. El volcanismo del Terciario superior del sur de Mendoza. Rev. Asoc. Geol. Argent. 57, 119–132.
Orchuela, I., Lara, M.E., Suarez, M., 2003. Productive large scale folding associated with igneous intrusions: El Trapial field, Neuquen Basin, Argentina. In: 2003 AAPG International Conference & Exhibition Technical Program.
Othman, R., Arouri, K.R., Ward, C.R., McKirdy, D.M., 2001. Oil generation by igneous intrusions in the northern Gunnedah Basin, Australia. Org. Geochem. 32, 1219–1232.
Ramos, V., 1978. Relatorio Geologico y Recursos Naturales del Neuquén. In: VII Congreso Geológico Argentino. Estructura, pp. 99.
Ramos, V.A., Folguera, A., 2005. Tectonic evolution of the Andes of Neuquén: constraints derived from the magmatic arc and foreland deformation. Geol. Soc. Lond. Spec. Publ. 252, 15–35.
Ramos, V.A., Vujovich, G., Martino, R., Otamendi, J., 2010. Pampia: a large cratonic block missing in the Rodinia supercontinent. J. Geodyn. 50, 243–255.
Rateau, R., Schofield, N., Smith, M., 2013. The potential role of igneous intrusions on hydrocarbon migration, West of Shetland. Petrol. Geosci. 19, 259–272.
Raymond, A., Murchison, D., 1991. The relationship between organic maturation, the widths of thermal aureoles and the thicknesses of sills in the Midland Valley of Scotland and Northern England. J. Geol. Soc. 148, 215–218.
Rossello, E.A., Cobbold, P.R., Diraison, M., Arnaud, N., 2002. Auca Mahuida (Neuquén basin, Argentina): a Quaternary shield volcano on a hydrocarbon-producing substrate. In: 5th International Symposium on Andean Geodynamics (ISAG 2002), Extended Abstracts, Toulouse, pp. 549–552.
Santos, R.V., Dantas, E.L., de Oliveira, C.G., de Alvarenga, C.J.S., dos Anjos, C.W.D., Guimarães, E.M., Oliveira, F.B., 2009. Geochemical and thermal effects of a basic sill on black shales and limestones of the Permian Irati Formation. J. S. Am. Earth Sci. 28, 14–24.
Schiuma, M.F., 1994. Intrusivos del valle del Río Grande, provincia de Mendoza, su importancia como productores de hidrocarburos. Facultad de Ciencias Naturales y Museo.
Schmiedel, T., Kjoberg, S., Planke, S., Magee, C., Galland, O., Schofield, N., Jackson, C.A.-L., Jerram, D.A., 2017. Mechanisms of overburden deformation associated with the emplacement of the Tulipan sill, mid-Norwegian margin. Interpretation 5, SK23–SK38.
Silvestro, J., Atencio, M., 2009. La cuenca cenozoica del río Grande y Palauco: edad, evolución y control estructural, faja plegada de Malargüe. Rev. Asoc. Geol. Argent. 65, 154–169.
Simoneit, B.R., Brenner, S., Peters, K., Kaplan, I., 1978. Thermal alteration of Cretaceous black shale by basaltic intrusions in the Eastern Atlantic. Nature 273, 501–504.
Simonet, B.R., Brenner, S., Peters, K., Kaplan, I., 1981. Thermal alteration of Cretaceous black shale by diabase intrusions in the Eastern Atlantic—II. Effects on bitumen and kerogen. Geochem. Cosmochim. Acta 45, 1581–1602.
Svensen, H., Planke, S., Malthe-Sørenssen, A., Jamtveit, B., Myklebust, R., Eidem, T.R., Rey, S.S., 2004. Release of methane from a volcanic basin as a mechanism for initial Eocene global warming. Nature 429, 542–545.
Svensen, H., Planke, S., Polozov, A.G., Schmidbauer, N., Corfu, F., Podladchikov, Y.Y., Jamtveit, B., 2009. Siberian gas venting and the end-Permian environmental crisis. Earth Planet Sci. Lett. 277, 490–500.
Svensen, H.H., Iyer, K., Schmid, D.W., Mazzini, A., 2017. Modelling of gas generation following emplacement of an igneous sill below Lusi, East Java, Indonesia. Mar. Petrol. Geol. https://doi.org/10.1016/j.marpetgeo.2017.07.007.
Sweeney, J.J., Burnham, A.K., 1990. Evaluation of a simple model of vitrinite reflectance based on chemical kinetics (1). AAPG Bull. 74, 1559–1570.
Sydnes, M., Fjeldskaar, W., Løtveit, I.F., Grunnaleite, I., Cardozo, N., 2018. The importance of sill thickness and timing of sill emplacement on hydrocarbon maturation. Mar. Petrol. Geol. 89, 500–514.
Sylwan, C., 2014. Source rock properties of Vaca Muerta Formation, Neuquina Basin, Argentina, Simposio de Recursos No Convencionales. In: IX Congreso Argentino de Exploración y Desarrollo de Hidrocarburos. IAPG, Mendoza, Argentina.
Thomaz Filho, A., Mizusaki, A.M.P., Antonioli, L., 2008. Magmatism and petroleum exploration in the Brazilian Paleozoic basins. Mar. Petrol. Geol. 25, 143–151.
Tunik, M., Folguera, A., Naipauer, M., Pimentel, M., Ramos, V.A., 2010. Early uplift and orogenic deformation in the Neuquén Basin: constraints on the Andean uplift from U–Pb and Hf isotopic data of detrital zircons. Tectonophysics 489, 258–273.
Uliana, M., Biddle, K., 1988. Mesozoic-Cenozoic paleogeographic and geodynamic evolution of southern South America. Rev. Bras. Geociencias 18, 172–190.
Uliana, M., Legarreta, L., 1993. Hydrocarbons habitat in a triassic-to-cretaceous sub-andean setting: Neuquén Basin, Argentina. J. Petrol. Geol. 16, 397–420.
Vergani, G.D., Tankard, A.J., Belotti, H.J., Welsink, H.J., 1995. Tectonic Evolution and Paleogeography of the Neuquén Basin, Argentina.
Wang, D., Manga, M., 2015. Organic matter maturation in the contact aureole of an igneous sill as a tracer of hydrothermal convection. J. Geophys. Res. Solid Earth 120, 4102–4112.
Wang, D., Song, Y., Xu, H., Ma, X., Zhao, M., 2013. Numerical modeling of thermal evolution in the contact aureole of a 0.9 m thick dolerite dike in the Jurassic siltstone section from Isle of Skye, Scotland. J. Appl. Geophys. 89, 134–140.
Witte, J., Bonora, M., Carbone, C., Oncken, O., 2012. Fracture evolution in oil-producing sills of the Rio Grande Valley, northern Neuquén Basin, Argentina. AAPG Bull. 96, 1253–1277.